

# Simple Maps with Fractal Diffusion Coefficients

R. Klages\*

*Institut für Theoretische Physik, Technische Universität Berlin, Sekr. PN 7-1,  
Hardenbergstr. 36, D-10623 Berlin, Germany*

J.R. Dorfman

*Institute for Physical Science and Technology and Department of Physics,  
University of Maryland, College Park, MD 20742, USA*

(November 23, 2018)

We consider chains of one-dimensional, piecewise linear, chaotic maps with uniform slope. We study the diffusive behaviour of an initially nonuniform distribution of points as a function of the slope of the map by solving the Frobenius-Perron equation. For Markov partition values of the slope, we relate the diffusion coefficient to eigenvalues of the topological transition matrix. The diffusion coefficient obtained shows a fractal structure as a function of the slope of the map. This result may be typical for a wide class of maps, such as two-dimensional sawtooth maps.

PACS numbers: 05.45.+b, 05.60.+w

The study of simple models for non-equilibrium processes in statistical physics has been one of the central themes in the theory of chaotic dynamical systems [1,2,3]. A great deal of work has been done to describe the large-scale motion in systems of independent particles each moving under the action of relatively simple maps, operating at discrete intervals of time. For one-dimensional sinusoidal, or piecewise differentiable maps, a variety of diffusive-like and ballistic-like behaviour has been studied [4,5,6,7]. For two-dimensional, conservative Hamiltonian maps, parameter dependent momentum-diffusion coefficients have been computed, often by a combination of numerical and analytical methods which explore the phase space structure of the dynamical system [8,9,10]. Recently, Gaspard and coworkers have established an explicit connection between fundamental quantities of dynamical systems, such as the Kolmogorov-Sinai entropy and Lyapunov exponents, and transport coefficients [11,12,13,14]. Related connections between transport coefficients and Lyapunov exponents have been discussed for non-equilibrium systems with thermostats [15]. There is also a close connection of the work described here to that based on periodic orbit expansions for transport coefficients [7,16].

In this letter, chains of piecewise linear, one-dimensional, chaotic maps

$$x_{\tau+1} = [x_{\tau}] + m_a(x_{\tau}) \equiv M_a(x_{\tau}) \quad (1)$$

will be considered, where  $\tau$  is the discrete time variable,  $[x_{\tau}]$  the largest integer smaller than  $x_{\tau}$ ,  $m_a(x_{\tau} + 1) = m_a(x_{\tau})$  represents a periodic function, and  $a$  stands for the control parameter, which is the slope of the map. We consider a chain of maps  $m_a(x_{\tau})$  with chainlength  $L$ . The absolute value of the slope is assumed to be uniform and its logarithm is equal to the Lyapunov exponent. We assume the maps are expanding, i.e. that  $|a| > 1$ .

Following the approach in [11,12,13,14], we describe a method by which the diffusion coefficient for this class of maps can be computed for a broad range of parameter values. The method will be illustrated by the map

$$m_a(x_{\tau}) := \begin{cases} ax_{\tau} & , \quad 0 < x_{\tau} \leq \frac{1}{2} \\ ax_{\tau} + 1 - a & , \quad \frac{1}{2} < x_{\tau} \leq 1 \end{cases} \quad , \quad a > 0 \quad , \quad (2)$$

as sketched in Fig. 1, which has been introduced and discussed in [3,4,13]. We find that the diffusion coefficient for this map shows a very rich fractal structure as a function of the slope.

To describe the dynamical behaviour of an arbitrary initial density for a set of particles on some interval of the line  $-\infty \leq x \leq \infty$ , we will need the Frobenius-Perron equation, supplemented by boundary conditions. The Frobenius-Perron equation is given by

$$\rho_{\tau+1}(x) = \int dy \rho_{\tau}(y) \delta(x - M_a(y)) \quad , \quad (3)$$

where  $\rho_{\tau}(x)$  is the probability density for points on the line, and  $M_a(y)$  is the map under consideration. We suppose that the motion takes place on an interval  $0 < x < L$ , and we impose periodic boundary conditions, i.e.  $\rho_{\tau}(0) = \rho_{\tau}(L)$  for all  $\tau$ , or absorbing boundary conditions  $\rho_{\tau}(x) = 0$  for  $x = 0, L$  for all  $\tau$  [17]. Next we use the argument of Gaspard and coworkers [11,12,13,14] to relate the eigenmodes of the Frobenius-Perron equation to the solution of the diffusion equation

$$\frac{\partial n(x,t)}{\partial t} = D \frac{\partial^2 n(x,t)}{\partial x^2} \quad , \quad (4)$$

where  $n(x,t)$  is the macroscopic density of particles at a point  $x$  at time  $t$ , and  $D$  is a diffusion coefficient. If

for large  $L$ , and large  $\tau$ , the first few eigenmodes of the Frobenius-Perron equation are identical to those of the diffusion equation, the diffusion coefficient can be obtained by matching eigenmodes in an appropriate scaling limit. More explicitly, for periodic boundary conditions  $n(0, t) = n(L, t)$ , one can easily see that for large times  $n(x, t)$  has the form

$$n(x, t) = \text{const.} + A \exp(-D(4\pi^2/L^2)t \pm i(2\pi/L)x) \quad . \quad (5)$$

Consequently, if one can find a solution of Eq. (3), for large  $L$  and  $\tau$ , in the form of

$$\rho(x, \tau) = \text{const.} + A' \exp(-\gamma_p(a)\tau \pm i(2\pi/L)x) \quad , \quad (6)$$

one can relate the decay rate  $\gamma_p(a)$  to  $D$  by

$$D(a) = \lim_{L \rightarrow \infty} (L/2\pi)^2 \gamma_p(a) \quad . \quad (7)$$

For absorbing boundary conditions one relates the diffusion coefficient to the escape rate from the system by an equation similar to Eq.(7). The escape-rate formalism of chaotic dynamics shows that the escape rate from a system with absorbing boundaries is equal to the Lyapunov exponent minus the Kolmogorov-Sinai entropy for particles trapped within the system whose trajectories lie on a fractal repeller [11]. For the case of maps with slopes of uniform magnitude considered here, the Komolgorov-Sinai entropy for the fractal repeller  $h_{KS}(a)$  is identical to the topological entropy of points on the repeller and it can be computed from  $\gamma_p(a)$  as  $h_{KS}(a) = \log a - \gamma_p/4 + O(L^{-3})$  [13].

The use of maps with uniform slope is not an essential ingredient in the calculation of  $D(a)$  described below, which can be applied to more general linear maps. The main idea is that the Frobenius-Perron equation can be written as a matrix equation whenever the parameters of the map are such that one can construct a Markov partition of the interval  $(0, L)$ , which has the property that partition points get mapped onto other partition points by the map  $M_a(x)$  [18]. In a related context, these partitions have been discussed in [19]. For such values of  $a$ , Eq.(3) can be written as

$$\boldsymbol{\rho}_{\tau+1} = (1/|a|) M \boldsymbol{\rho}_\tau \quad , \quad (8)$$

where  $\boldsymbol{\rho}_\tau$  is a column vector of the probability densities in each of the Markov partition regions at time  $\tau$ , and  $M$  is a topological transition matrix whose elements  $M_{ij}$  are unity if points in region  $j$  can be mapped into region  $i$ , and are zero otherwise.

As a simple example we consider the form of the matrix  $M$  when  $a = 3$ , the map  $M_a(x)$  is given by Eqs.(1),(2), and periodic boundary conditions are used on an interval of length  $L$ . In this case the regions of the partition are

all of length  $1/2$ , as illustrated in Fig. 1. Then  $M$  is a  $2L \times 2L$  matrix of the form

$$M = \begin{pmatrix} 1 & 1 & 0 & 0 & \cdots & 0 & 0 & 1 & 0 \\ 1 & 1 & 0 & 1 & 0 & 0 & \cdots & 0 & 0 \\ 1 & 0 & 1 & 1 & 0 & 0 & \cdots & 0 & 0 \\ 0 & 0 & 1 & 1 & 0 & 1 & 0 & 0 & \cdots \\ 0 & 0 & 1 & 0 & 1 & 1 & 0 & 0 & \cdots \\ \vdots & & & & \vdots & & & \vdots & \\ 0 & 1 & 0 & 0 & \cdots & 0 & 0 & 1 & 1 \end{pmatrix} \quad . \quad (9)$$

In the limit  $\tau \rightarrow \infty$ , for any  $L$ , and any ‘‘Markov partition’’ value of  $a$ , the Frobenius-Perron equation can be solved in terms of the eigenmodes of  $M$  for any initial value  $\rho_0(x)$  which is uniform in each of the Markov partition regions. For periodic boundary conditions,  $M$  is always a (block)circulant [20], the largest eigenvalue of  $M$  is precisely  $|a|$ , and the corresponding eigenmode is a constant, representing the equilibrium state. The rate of decay to equilibrium,  $\gamma_p(a)$ , is obtained as  $\gamma_p(a) = \log(|a|/\chi_1)$ , where  $\chi_1$  is the next largest eigenvalue of  $M$  [13]. Analytical expressions for  $D(a)$  can be derived for all integer values of  $a \geq 2$ . For even integers, the results of Grossmann and Fujisaka [4] are recovered,  $D(a) = (1/24)(a-1)(a-2)$ , and for odd integers we find  $D(a) = (1/24)(a^2-1)$ . To obtain  $D(a)$  for a general Markov partition value of  $a$ , one can use computer methods [21].

Fig. 2 (a) shows the results for the diffusion coefficient of the dynamical system Eqs.(1),(2) for values of  $a$  in the range  $2 \leq a \leq 8$ . In Fig. 2 (b)-(d), we present magnifications of three small regions in this interval [22]. One can see clearly that  $D(a)$  has a complicated fractal structure with regions exhibiting self-similarity. In Fig. 3, we show an enlargement of the region for  $2 \leq a \leq 3$ . The dashed line is the prediction of  $D(a)$  for a simple random-walk model suggested by Schell, Fraser and Kapral [5]. Note that the model correctly accounts for the behaviour of  $D(a)$  near  $a = 2$ . The wiggles in this graph can be understood by considering the transport of particles from one unit interval to another. These regions are coupled to each other by *turnstile*s, where points in one unit interval get mapped outside that particular interval into another unit interval. As in the case of two-dimensional twist maps, such as the sawtooth map, these turnstiles are crucial for large-scale transport [2,23].

The region  $2 \leq a \leq 3$  can be analyzed by studying the interaction of turnstiles [24]. One can recognize three distinct series of values of  $a$ , each of which provides a cascade of apparently self-similar regions of decreasing size, as the limits  $a \rightarrow 2$  or  $a \rightarrow 3$  are approached. To understand these series, consider the trajectory of a point that starts just to the left at  $x = 1/2$ . The first iterate of  $x = 1/2$  is in the second interval,  $(1, 2)$ . The *series  $\alpha$*  values of  $a$  are defined by the condition that the second iterate of  $x = 1/2$  is at the leftmost point of the upward

turnstile in the second interval (1, 2) ( $a = 2.732$ ), or that the third iterate is at the corresponding point in the third interval ( $a = 2.920$ ), etc. The numbers on the graph refer to the number of intervals the image of  $x = 1/2$  has travelled before it gets to the appropriate point on the turnstiles. *Series  $\beta$*  points are defined in a similar way, but they are allowed to have two or more internal reflections within an interval before reaching the left edge of a turnstile. *Series  $\gamma$*  points are defined by the condition that some image of  $x = 1/2$  has reached the rightmost edge of an upward turnstile (i.e. some point  $x = n + 1/2$ , where  $n$  is an integer), and consequently an increase in  $a$  will lead to a decrease in  $D(a)$ . These cascades provide a basis for a physical understanding of the features of  $D(a)$  in this region: Particles leave a particular unit interval through a turnstile and undergo a number of iterations before they are within another turnstile. Whether they continue to move in the same or the reverse direction at the next and later turnstiles is a sensitive function of the slope of the map. Thus the fractal structure of the  $D(a)$  curve is due to the effects of long-range correlations among turnstiles and these correlations lead to changes of  $D(a)$  on an infinitely fine scale. A similar argument can be employed to explain, at least qualitatively, the fractal structure of  $D(a)$  for higher values of the slope, although more work needs to be done before a full understanding of this curve is obtained [25].

We conclude with a few remarks: (A) Our results appear to be the first example of a system whose diffusion coefficient has an unambiguously fractal structure. We suspect that similar results obtain for all other one-dimensional, piecewise linear maps [26], which might be of interest, e.g., for chaotic scattering [27], as well as for transport in maps of more than one dimension, such as sawtooth maps. We note that oscillations of the diffusion coefficient with respect to an appropriate control parameter, which could be a field strength, have already been found in the standard [8] and the sawtooth map [10]. (B) It is not known whether this fractal structure persists for smooth maps where the function  $M_a(x)$  is  $C^1$ , or where the map contains some randomness. (C) We have numerical evidence that the Markov points are dense for  $a \geq 2$ , and we believe that our results give the full structure of the  $D(a)$  function. Nevertheless, it would be valuable to have a mathematical proof.

We are indebted to J. Yorke for an important hint regarding Markov partitions. Helpful discussions with Chr. Beck, C. Grebogi, R. Kapral, L. Bunimovich, and B. Hunt are gratefully acknowledged. R.K. wants to thank the Institute for Physical Science and Technology for its hospitality, and he is grateful to S. Hess, T.R. Kirkpatrick, the DAAD and the NaFöG commission Berlin for financial and other support.

\* e-mail: rkla0433@w421rzr.physik.tu-berlin.de

- [1] H.G. Schuster, *Deterministic Chaos* (VCH Verlagsgesellschaft mbH, Weinheim, 1989), 2nd edition; A.J. Lichtenberg, M.A. Lieberman, *Regular and Chaotic Dynamics*. (Springer, New York, 1983) 2nd edition; M. Mareschal, B.L. Holian eds., *Microscopic Simulations of Complex Hydrodynamic Phenomena* (Plenum, New York, 1992)
- [2] S. Wiggins, *Chaotic Transport in Dynamical Systems* (Springer-Verlag, New York, 1992)
- [3] E. Ott, *Chaos in Dynamical Systems* (Cambridge, 1993)
- [4] S. Grossmann, H. Fujisaka, Phys.Rev. A **26**, 1179 (1982); H. Fujisaka, S. Grossmann, Z.Phys. B - Condensed Matter **48**, 261 (1982)
- [5] M. Schell, S. Fraser, R. Kapral, Phys.Rev. A **26**, 504 (1982)
- [6] T. Geisel, J. Nierwetberg, Phys.Rev.Lett. **48**, 7 (1982); S. Grossmann, S. Thomae, Phys.Lett. **97A**, 263 (1983); T. Geisel, S. Thomae, Phys.Rev.Lett. **52**, 1936 (1984); T. Geisel, J. Nierwetberg, A. Zacherl, Phys.Rev.Lett. **54**, 616 (1985)
- [7] R. Artuso, Phys.Lett. A **160**, 528 (1991); R. Artuso, G. Casati, R. Lombardi, Phys.Rev.Lett. **71**, 62 (1993)
- [8] A.B. Rechester, R.B. White, Phys.Rev.Lett. **44**, 1586 (1980); A.B. Rechester, M.N. Rosenbluth, R.B. White, Phys.Rev. A **23**, 2664 (1981)
- [9] J.R. Cary, J.D. Meiss, A. Bhattacharjee, Phys.Rev. A **23**, 2744 (1981); J.R. Cary, J.D. Meiss, Phys.Rev. A **24**, 2664 (1981); T.M. Antonsen, E. Ott, Phys.Fluids **24**, 1635 (1981)
- [10] I. Dana, N.W. Murray, I.C. Percival, Phys.Rev.Lett. **62**, 233 (1989); I. Dana, Physica D **39**, 205 (1989)
- [11] P. Gaspard, G. Nicolis, Phys.Rev.Lett. **65**, 1693 (1990)
- [12] J.R. Dorfman, P. Gaspard, submitted to Phys.Rev. E
- [13] P. Gaspard, J.Stat.Phys. **68**, 673 (1992); Phys.Lett. A **168**, 13 (1992); Chaos **3**, 427 (1993)
- [14] P. Gaspard, F. Baras, in *Microscopic Simulations of Complex Hydrodynamic Phenomena*. op.cit.
- [15] D.J. Evans, E.G.D. Cohen, G.P. Morris, Phys.Rev. A **42**, 5990 (1990); A. Baranyai, D.J. Evans, E.G.D. Cohen, J.Stat.Phys. **70**, 1085 (1993); N.I. Chernov *et al.*, Phys.Rev.Lett. **70**, 2209 (1993); Comm.Math.Phys. **154**, 569 (1993); H.A. Posch, W.G. Hoover, Phys.Lett. A **123**, 227 (1987); Phys.Rev. A **39**, 2175 (1989)
- [16] P. Cvitanović, J.-P. Eckmann, P. Gaspard, Niels Bohr Institute preprint (May 1991); P. Cvitanović, P. Gaspard, T. Schreiber, Chaos **2**, 85 (1992), and references therein
- [17] N.G.v. Kampen, *Stochastic Processes in Physics and Chemistry* (North Holland, Amsterdam, 1981)
- [18] see, e.g., A. Boyarski, M. Skarowsky, Trans.Am.Math. Soc. **225**, 243 (1979); A. Boyarski, J.Stat.Phys. **50**, 213 (1988); Chr. Beck, F. Schlögl, *Thermodynamics of Chaotic Systems* (Cambridge, 1993)
- [19] C.S. Hsu, M.C. Kim, Phys.Rev. A **31**, 3253 (1985); N. Balmforth, E.A. Spiegel, C. Tresser, Phys.Rev.Lett. **72**, 80 (1994)
- [20] see, e.g., T.H. Berlin, M. Kac, Phys.Rev. **86**, 8211 (1952); Ph.J. Davis, *Circulant Matrices* (Wiley, New York, 1979)
- [21] For circulant matrices, standard software packages (NAG, IMSL) do not always give the full spectrum correctly (cf. R.M. Beam, R.F. Warming, NASA Technical Memorandum 103900 (Moffett Field, California, 1991), unpublished), but the results for the first two largest eigenvalues

are reliable.

- [22] For a chainlength of  $L = 100$ , the numerical precision for each  $D(a)$  is always better than 0.1% with respect to the limit in Eq.(7). Therefore, errorbars do not appear in the diagrams.
- [23] R.S. Mackay, J.D. Meiss, I.C. Percival, *Physica D* **13**, 55 (1984), Q. Chen, J.D. Meiss, *Nonlinearity* **39**, 347 (1989); Q. Chen *et al.*, *Physica D* **46**, 217 (1990); J.D. Meiss, *Rev.Mod.Phys.* **64**, 795 (1992)
- [24] R. Klages, J.R. Dorfman, in preparation
- [25] These qualitative explanations are not sufficient to get the exact values for all the local extrema of  $D(a)$ . Compare, e.g.,  $a = 3, 5, 7, \dots$
- [26] After this letter was submitted we were informed that related results, based on the methods of Ref. [16], have been obtained for another one-dimensional map by H.-C. Tseng *et al.*, submitted to *Phys. Lett. A*.
- [27] Y.-Ch. Lai, C. Grebogi, *Phys.Rev. E* **49**, 3761 (1994); Y.-Ch. Lai *et al.*, *Phys.Rev.Lett.* **71**, 2212 (1993)

FIG. 1. Illustration of the dynamical system Eqs. (1),(2) for a particular slope,  $a = 3$ . The Markov partition given by the dashed grid leads to the construction of the transition matrix in Eq. (9).

FIG. 2. Diffusion coefficient  $D(a)$  computed for the dynamical system Eqs. (1),(2) and some enlargements. Graph (a) consists of 7908 single data points. In graph (b)-(d), the dots are connected with lines. The number of data points is 476 for (b), 1674 for (c), and 530 for (d).

FIG. 3. Enlargement of the region of slope  $a \leq 3$  with the solution for a simple random walk model (dashed line) and labels for the values which are significant for “turnstile dynamics” (see text). For some points, the turnstile coupling is shown by pairs of boxes. The graph shows 979 single data points.

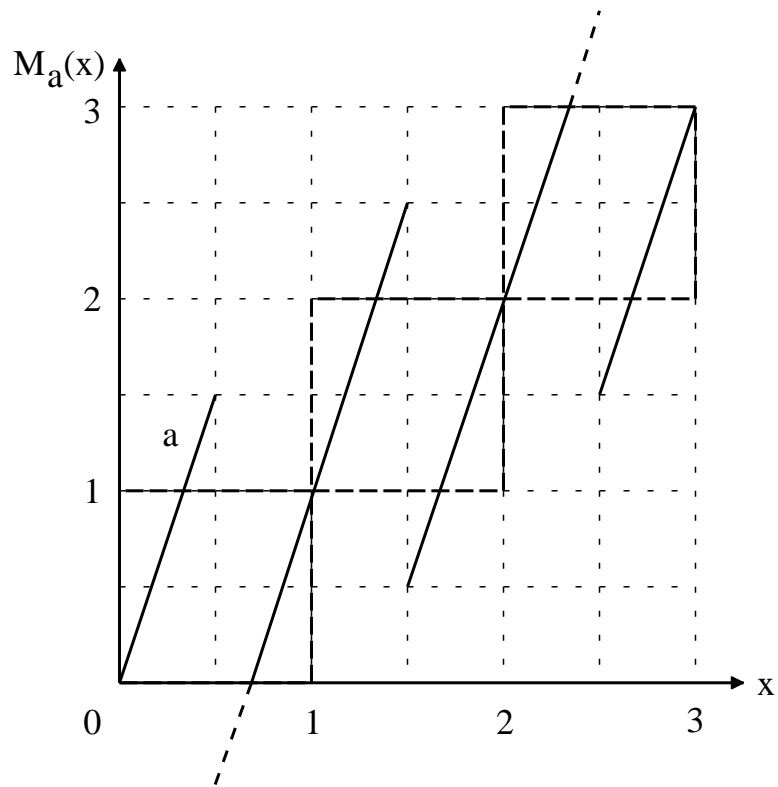


Figure 1

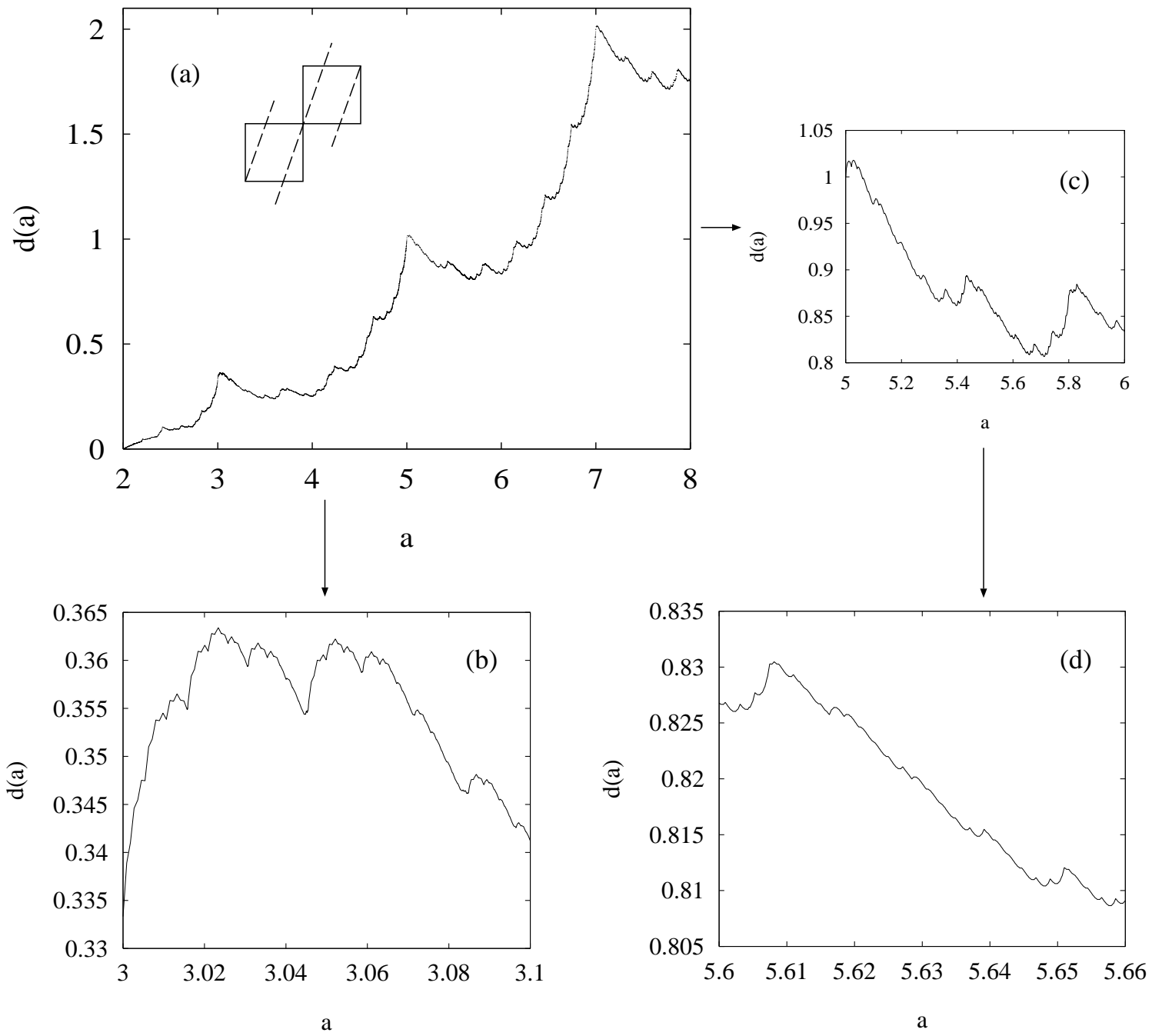


Figure 2

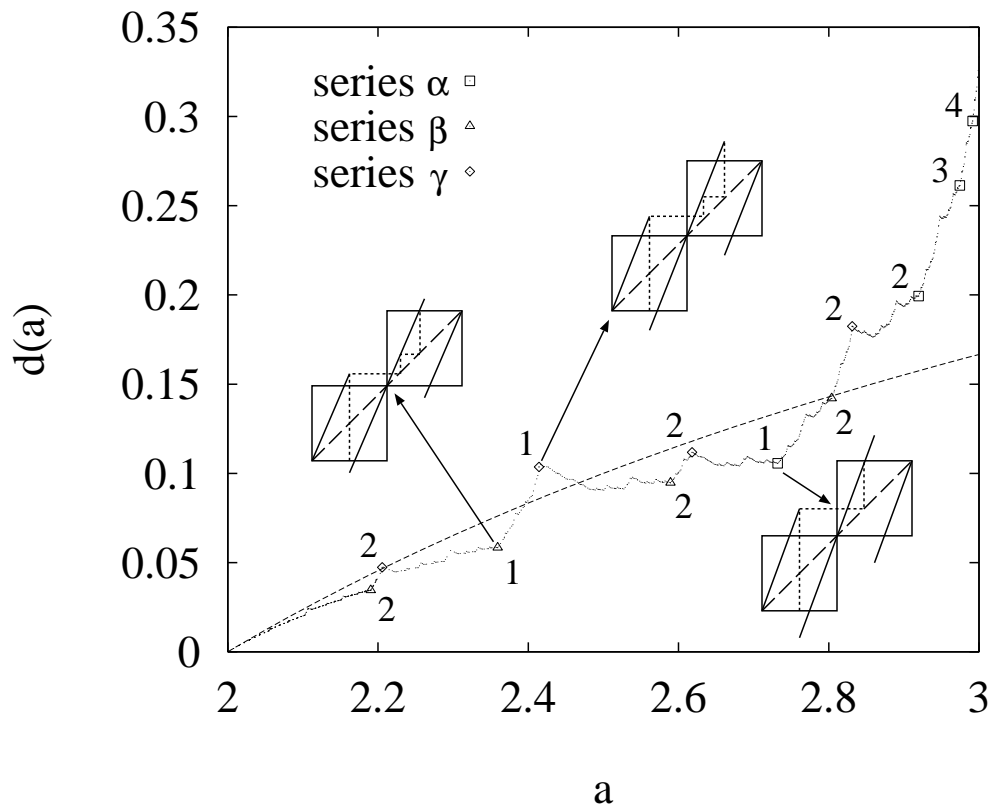


Figure 3